

Microwave-assisted synthesis of chitosan-hydroxyapatite composite from eggshells and its adsorption properties

Meta F. Rizkiana*, Zakia A. Salsabila, Rana I. Aulia, Helda W. Amini, Bekti Palupi, Istiqomah Rahmawati, Boy A. Fachri

Research Center for Bio-based Chemical Products, Department of Chemical Engineering, Faculty of Engineering, Universitas Jember, Jember 68121 Indonesia

*Corresponding author, e-mail: metafitririzkiana@unej.ac.id

Received 15 Dec 2022, Accepted 5 Mar 2024
Available online 21 Jul 2024

ABSTRACT: One of the successful methods for dye removal is adsorption. Utilizing eggshells as a bioadsorbent is an interesting approach to decrease negative environmental impacts and improve the economic value of this waste material. Hydroxyapatite (HA) is a valuable biomaterial that can be derived from chicken eggshells using microwave irradiation synthesis. This study combined chitosan (CS) with HA using the precipitation method to develop CS-HA composite, a promising adsorbent with high adsorption capacity for dyes. Scanning electron microscopy (SEM) and Fourier transform infrared spectroscopy (FTIR) were conducted to determine the composite biomaterials' morphology and functional groups. The results showed that the biomaterials particles exhibit a grain-like morphology with agglomerated spherical-shaped nanoparticles. The characteristic functional groups corresponding to HA and CS were identified and disclosed the successful synthesis of a biocomposite, the CS-HA. Adsorption capacity toward methylene blue of the CS-HA was investigated to discover its adsorption properties. The results showed that the equilibrium adsorption capacity of CS-HA was 11.0 mg/g, and its adsorption isotherm model was consistent with the Freundlich adsorption model. In addition, thermodynamic tests confirmed that the adsorption process of CS-HA was exothermic and spontaneous, with superior adsorption performance at low temperatures.

KEYWORDS: microwave synthesis, hydroxyapatite composites, eggshells, methylene blue removal, adsorption

INTRODUCTION

Wastewaters from various industries, including textile, cosmetic, rubber, pharmaceutical, food, and paint industries, release hazardous substances, such as synthetic dyes, suspended solids, and organic compounds. These dye molecules are stable and difficult to decompose. The carcinogenic materials in organic dyes can threaten humans and the aquatic environment. Therefore, properly treating dyes in wastewater is required to maintain the environmental ecosystem [1]. Synthetic dyes are classified into three categories: anionic, cationic, and nonionic. As our focus in this adsorption study, methylene blue is a commonly used dye, soluble in water, and challenging to remove due to its complicated structure [2]. Methylene blue belongs to the cationic class as it dissociates as chloride ions and cations in aqueous solutions [3, 4].

Researchers have employed several methods to remove dye waste, including chemical treatments (photocatalytic [5, 6], oxidation [7], coagulation [8, 9]), biological treatments [10, 11], and physical treatments using ultrafiltration [12] and adsorption [13, 14]. Adsorption is a practical method used for dye removal. It is an effective technique for dealing with industrial wastewater problems because the process of adsorption can reduce the dye concentration in the solution and eliminate odors. Adsorption methods involve mass transfer between solids from bulk liquid to the surface of adsorbents [15]. The advantages of adsorbents

include their high surface area, high porosity, high affinity to pollutants, and ease of fabrication. Adsorbents can be classified into two categories: organic and inorganic [16]. Several adsorbents, such as activated carbon [17], silica ash, metal-oxide-based [18], carbon-based [19], polymer-based [20], metal-organic framework (MOF) [21], and hydroxyapatite [22] have been applied for dye removal.

The molecular formula of hydroxyapatite (HA), or calcium hydroxy phosphate, is $\text{Ca}_{10}(\text{PO}_4)_6(\text{OH})_2$. HA is biocompatible, biodegradable, low-toxic, with a high adsorption capacity [23]. It can be obtained from natural or synthetic materials. The fabrication of synthetic HA requires high expenditure due to the usage of high-purity reagents. Hence, preparation from natural sources or wastes such as eggshells will be beneficial [24]. Eggshell is the outermost layer of an egg, and its hard texture protects the egg's contents from environmental conditions. The main content of eggshells is calcium carbonate (CaCO_3) of around 80–95%, varied widely depending on types of eggs. Eggshells can be used as a precursor for producing HA [25]. Several researchers have utilized and processed eggshell wastes into HA. In the adsorption application, the mechanisms rely on the surface hydroxyl group (–OH), which is the binding species to create strong interaction with pollutants [4]. Meanwhile, chitosan (CS) is a natural polysaccharide used as a dye adsorbent to remove dyes. It possesses hydroxyl (–OH) and amino (–NH₂) groups as binding sites [26] to

form hydrogen bonding with methylene blue [3]. It is often combined with other materials to overcome its limitations, such as high solubility in acids, difficulty separating, weak mechanical properties, and easy-to-form gel characteristics [27]. This study combined HA and CS biopolymer to develop a more versatile and robust adsorbent material.

The common methods to synthesize HA include freeze drying [28, 29], wet chemical methods, sol-gel, calcination, and hydrothermal methods [24]. This study used a novel approach for fabricating composite of CS-HA. Microwave irradiation was used to enhance the chemical reactions involved in the synthesis of HA from eggshells as a source of calcium. This method was selected due to its efficiency and economic advantages [30]. The present study aimed to prepare HA nanocomposites with CS biopolymer to study their morphology and adsorption properties toward methylene blue.

MATERIALS AND METHODS

Materials

Eggshells were collected from food street vendors near Universitas Jember, Jember, Indonesia. CS (90% deacetylated form), methylene blue, sodium hydroxide (NaOH), ethanol, nitric acid (HNO_3) (65%), ammonium hydroxide (NH_4OH) (25%), acetic acid (CH_3COOH) (96%), and phosphoric acid (H_3PO_4) (85%) were purchased from Merck, Germany. All of the chemical reagents were of analytical grade.

Preparation of HA from eggshells

The preparation of HA referred to previous studies from Holloman et al [31]. The pre-treatment process started by cleaning the eggshells from impurities with clean water and boiling them in deionized water for 24 h. Next, the eggshells were ground to a fine powder and passed through a 100-mesh sieve; hence, fine eggshell powder, or CaCO_3 powder, was obtained. HA was then prepared by stirring a calcium solution (20 g of CaCO_3 powder dissolved in 28 ml HNO_3) at 300 rpm for 30 min in an Erlenmeyer flask to produce a pale yellow $\text{Ca}(\text{NO}_3)_2$. Next, 3 g of $\text{Ca}(\text{NO}_3)_2$ was dissolved in 100 ml of deionized water and stirred at 400 rpm for 10 min at 40 °C.

A phosphate solution was then prepared by mixing 60 ml of NH_4OH with 15 ml of H_3PO_4 at a speed of 1 ml/min using a micropipette. The resulting precipitate, which was $(\text{NH}_4)_2\text{HPO}_4$, was washed using deionized water and ethanol in a ratio of 1:1. Then, 2.4 g of $(\text{NH}_4)_2\text{HPO}_4$ was dissolved in 60 ml of deionized water to obtain the phosphate solution. The synthesis process began by adding the phosphate solution to the $\text{Ca}(\text{NO}_3)_2$ solution drop by drop. The pH of the mixed solution was adjusted to pH 11 using NH_4OH and stirred for 5 min. The mixed solution was then placed into a microwave (15 min, 450 W,

2.45 GHz, 80 °C). Once the mixed solution cooled down, an aging process was continued at room temperature for 24 h. The precipitate was then washed with distilled water and ethanol in a ratio of 1:1 (50:50 v/v) to remove the remaining ammonium nitrate and centrifuged to remove residual polymers and ammonium nitrate. The washing process was repeated three times. The washed precipitate of HA was then filtered and dried in an oven at 105 °C for 2 h.

Preparation of chitosan-hydroxyapatite composites (CS-HA)

To prepare the CS-HA composite, two different solutions were first prepared. The first solution was made by mixing CS with 2% acetic acid, and the second solution by mixing HA powder with 2% acetic acid with an overall ratio of 1:1, i.e. the first and second solutions are present in equal mass and volume. Each solution was then stirred using a magnetic stirrer with a stirring speed of 300 rpm at 37 °C for 4 h until homogeneous. Next, 10% NaOH was added until the pH of the solutions changed to pH 9.5, and a precipitation was observed. The resulting precipitate was washed with distilled water until the pH was neutral and, then, dried in an oven at 105 °C for 2 h [32].

Characterization of CS-HA

The morphology of CS-HA was investigated using scanning electron microscopy (SEM). The functional groups in the adsorbents were analyzed using Fourier transform infrared (FTIR) spectroscopy within the range of 4000–450 cm^{-1} .

Adsorption experiments

A stock solution of methylene blue (MB) solution (1000 mg/l) was prepared by dissolving the required amount with demineralized water. MB solutions with concentrations of 5 to 50 mg/l were prepared by diluting the stock solution. All adsorption tests were performed in a 100 ml stopper Erlenmeyer flask. The flask was shaken at 120 rpm in a temperature-controlled incubator and a natural pH (pH 7.73 for MB). The adsorption experiments were conducted by mixing 100 mg of CS-HA with 100 ml of the MB solution of different initial concentrations (5–50 mg/l) in a 100 ml stopper Erlenmeyer flask at different temperatures between 35 °C and 45 °C. The mixtures were shaken at 120 rpm for 24 h. Subsequently, the mixtures were centrifuged for 10 min at 1500 rpm to separate the filtrate and the adsorbent. The filtrate concentration of each mixture was measured (MB adsorption wavelengths = 665 nm) using a UV/vis spectrophotometer. The adsorption capacity at equilibrium q_e in mg/g was calculated using Eq. (1).

$$q_e = \frac{(C_0 - C_e)V}{1000 \times M_{\text{CS-HA}}} \quad (1)$$

where C_0 and C_e were the initial and the equilibrium concentrations (mg/l) of the MB solution, V was the volume of the MB solution (ml), and $M_{\text{CS-HA}}$ was the mass of the added CS-HA.

The adsorption isotherm parameters for MB were investigated, and the experimental data were fitted with the Langmuir and Freundlich isotherm model equations. Furthermore, the adsorption by CS-HA was examined thermodynamically for the removal of MB from an aqueous solution. Finally, thermodynamic parameter calculations were conducted.

RESULTS AND DISCUSSION

Morphologies of CS-HA

Characterization of the HA and the CS-HA was observed using scanning electron microscopy (SEM) with magnifications of 250 \times , 500 \times , 750 \times , and 1000 \times . The morphologies of HA were shown in Fig. 1. The SEM images indicated that HA was successfully synthesized and formed highly agglomerated spheres. The spherical-shaped particles with clumped distributions were visible from the SEM analysis. The agglomerated grains of HA were similar to the report by Chandrasekaran et al [33]. The addition of CS influenced the morphology of HA. Fig. 2 shows the SEM images of the CS-HA composite. After adding CS, a cauliflower-like appearance was observed in the composite. CS could envelop the HA particles forming interconnected beads. Due to the presence of CS, the initially small HA spheres tended to gather into lumps. The porosity in CS-HA was denser with the addition of CS.

Fourier transform infrared spectroscopy of CS-HA

The FTIR characterization step aimed to determine the functional groups of compounds. Fig. 3 represents the FTIR spectra of HA and CS-HA. The FTIR analysis of HA showed several functional groups, including OH⁻, PO₄³⁻, and O–P–O. The intense absorption peak at 1026 cm⁻¹ was ascribed to the stretching vibration of phosphate groups (PO₄³⁻). The bands at 600 and 561 cm⁻¹ corresponded to the bending vibration of O–P–O phosphate groups [28]. The broad peak at 3349 cm⁻¹ was assigned to the stretching vibration of the –OH group.

Furthermore, the intense adsorption peak in the CS-HA composite resulted from the PO₄³⁻ group observed at 1022 cm⁻¹, and the adsorption peaks at 598 cm⁻¹ and 559 cm⁻¹. For the CS-HA, the –OH stretch was shown in the peak at 3304 cm⁻¹. The difference in the intensity of the –OH group between HA and CS-HA indicated an increase in the concentration of the functional group. The increase of OH groups suggested a successful formation of the CS-HA composite between HA and CS. The obtained bands at 1643 cm⁻¹ could be assigned as the C–N–H of CS. Moreover, the bands presented at 1553 cm⁻¹ could be attributed to

Table 1 The adsorption isotherm parameters of MB on the CS-HA composites.

Isotherm model	Temp.	Parameter	Value
Langmuir	35 °C	q_m (mg/g)	–15.311
		K_L (l/mg)	-1.216×10^{-5}
		R^2	0.984
	45 °C	q_m (mg/g)	–3.464
		K_L (l/mg)	-2.987×10^{-5}
		R^2	0.930
Freundlich	35 °C	K_F	0.162
		$1/n$	1.151
		R^2	0.951
	45 °C	K_F	0.076
		$1/n$	1.423
		R^2	0.870

NH₂ bending [34]. The bands at 1410 cm⁻¹ and 1150 cm⁻¹ corresponded to the C–H vibration and C–O–C linkage, respectively. Finally, the C–N fingerprint band appeared at 873 cm⁻¹ [35]. Overall, the characteristic bands of HA and CS could be observed in the FTIR spectra of CS-HA.

OH, NH₂, Ca³⁺, and PO₄³⁻ contributed to the bonding between CS and HA. The OH band at 3349 cm⁻¹ shifted to the lower band at 3304 cm⁻¹, which could explain the interaction between CS-HA, suggesting that the Ca³⁺ attached to the NH₂ and the OH groups of CS. The oxygen of PO₄³⁻ was coordinated with N–H of CS, resulting in the peak at 1026 cm⁻¹ shifted to a lower band at 1022 cm⁻¹. Oxygen of PO₄³⁻ interacted with the NH₂ group of CS, resulting in a decreasing hydrophilicity of the CS [34].

The adsorption isotherm of MB on CS-HA

The adsorption isotherm experiment was conducted to investigate the maximum equilibrium concentration of MB on CS-HA composites and their adsorption behavior. The experimental data were assessed with the Langmuir and Freundlich isotherm model.

Langmuir equation:

$$\frac{1}{q_e} = \frac{1}{q_m K_L C_e} + \frac{1}{q_m} \quad (2)$$

Freundlich equation:

$$\ln q_e = \ln K_F + \frac{1}{n} \ln c_e \quad (3)$$

where q_e is the amount of MB adsorbed at equilibrium (mg/g) and c_e is the equilibrium concentration of dye solutions. In the Langmuir equation, q_m (mg/g) indicates adsorption capacity under experimental conditions and K_L is a constant related to the adsorption energy. The Freundlich parameters consist of $1/n$, the

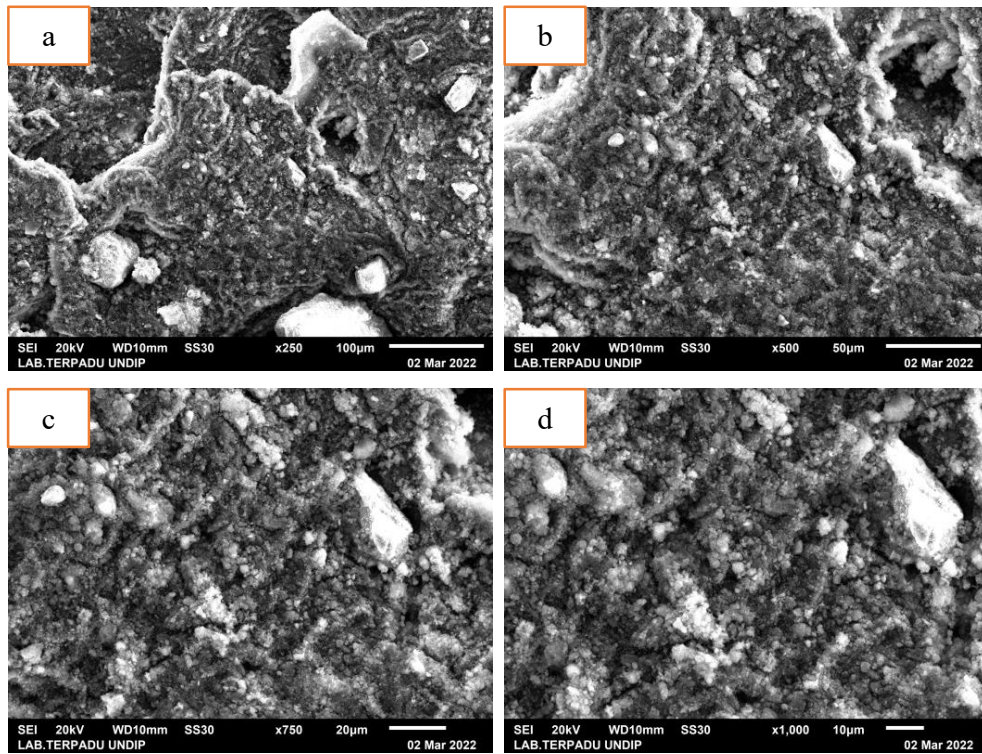


Fig. 1 SEM images of hydroxyapatite (HA): (a), 250×; (b), 500×; (c), 750×; and (d), 1000×.

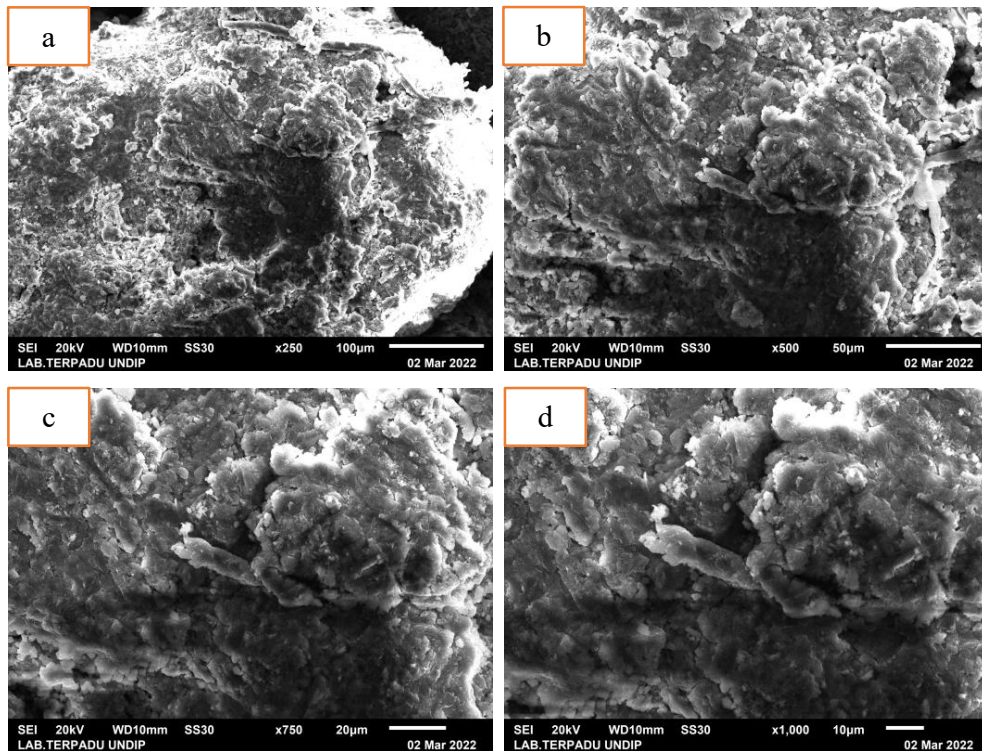


Fig. 2 SEM images of CS-HA composites: (a), 250×; (b), 500×; (c), 750×; and (d), 1000×.

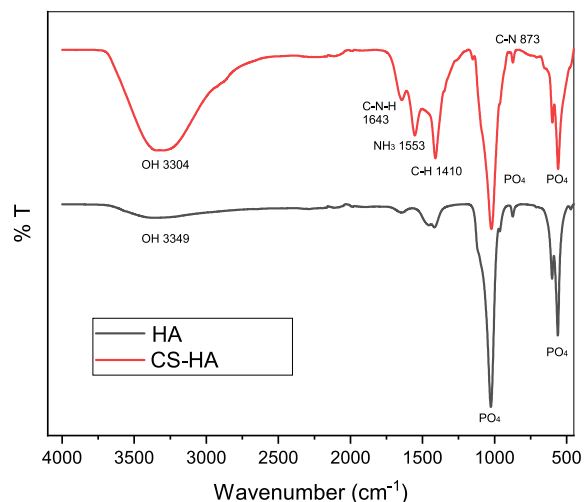


Fig. 3 FTIR result of HA and CS-HA composites.

Freundlich exponent; and K_F is related to adsorption capacity [36].

The graphs of the two isotherm models and the calculated parameter were shown in Fig. 4 and Table 1, respectively. The values of R^2 were considered reliable with experimental data if it is higher than 0.9. The graph of the Langmuir and Freundlich model with a temperature of 35 °C showed that the experimental data had a good fit with the Freundlich isotherm model, and the R^2 value was 0.9508. Although the R^2 value of the Langmuir model was larger (more linear), it did not follow the Langmuir isotherm model due to the negative results in q_m and K_L . The negative results reflected the inadequacy of Langmuir model for describing the adsorption mechanism [37]. Similar results were obtained at a temperature of 45 °C, where the Freundlich regression value R^2 was 0.8698.

The critical parameters for Freundlich isotherm were n , which indicates adsorption intensity; and K_F , which was related to adsorption capacity. The maximum adsorption capacity of MB by the adsorbent CS-HA composite was calculated as:

$$q_e = K_f c_e^{1/n} \quad (4)$$

Based on the equation, the maximum adsorption capacity of MB was 11.0 mg/g. The calculated n value for the adsorption of MB was 0.8691, indicating good efficiency for MB adsorption by the CS-HA composite. Freundlich isotherm describes the adsorption of a single adsorbate in solution as a reversible equilibrium. The Freundlich isotherm model states that non-uniform multilayers of adsorbate can be formed on the surface of adsorbent. The surface sites are heterogeneous, and there are intermolecular forces between adsorbates. The surface of CS-HA had evenly distributed hydroxyl and amine groups supporting hydrogen bonding interaction between the MB and the adsorbent.

Table 2 The adsorption thermodynamic parameters of MB on the CS-HA composites.

MB concentration (mg/l)	ΔH^0 (kJ/mol)	ΔS^0 (kJ/mol)	ΔG^0 (kJ/mol)	
			35 °C	45 °C
10	-35.516	-0.110	-35.934	-35.944
20	-35.055	-0.107	-1.921	-0.846
30	-55.137	-0.171	-2.319	-0.606

The adsorption thermodynamic of MB on CS-HA

Adsorption thermodynamic parameters such as enthalpy, Gibb's energy, and entropy were calculated. Table 2 shows the enthalpy value (ΔH) < 80 kJ/mol, meaning that the adsorption process was physisorption or physical adsorption. Enthalpy values were negative, indicating that the adsorption process was exothermic or heat releasing. The exothermic reaction in the adsorption process occurs when the adsorbate molecules interact with the surface of the adsorbent, releasing a certain amount of energy. The exothermic adsorption process showed that the adsorption capacity of CS-HA decreased as the temperature increased. Increasing the temperature improved the solubility of adsorbate in solvent (water).

The entropy (ΔS) value aims to determine the level of disorder in the adsorption process. Table 2 shows that the entropy value was negative, implying a decrease in the irregularity between the surface of the CS-HA and the MB during the adsorption process. Meanwhile, when MB was absorbed into the CS-HA, there was a reduction in the free movement of the MB molecules.

The value of Gibb's free energy (ΔG) aims to determine the total entropy change in a reaction. Table 2 shows that the value of ΔG was negative for both temperatures, indicating that the adsorption process of MB on the CS-HA composite occurred spontaneously. A higher negative value of ΔG showed the higher adsorption capacity possessed by an adsorbent. The value of the change in free energy for the physical adsorption process in this study, as shown in Table 2, indicated that the adsorption process was more favorable at low temperatures. Overall, the negative values for all thermodynamic parameters, such as enthalpy (ΔH), entropy (ΔS), and ΔG , explain that the adsorption process of MB by the CS-HA composite is spontaneous and more favorable at low temperatures.

CONCLUSION

A CS-HA composite was fabricated in this study. Its morphology, functional groups, and adsorption behavior on MB were studied. The experimental data confirmed that the composite has the potential to remove MB from aqueous solution. Langmuir and Freundlich adsorption isotherms were employed to study the composite's adsorption behavior, and the ex-

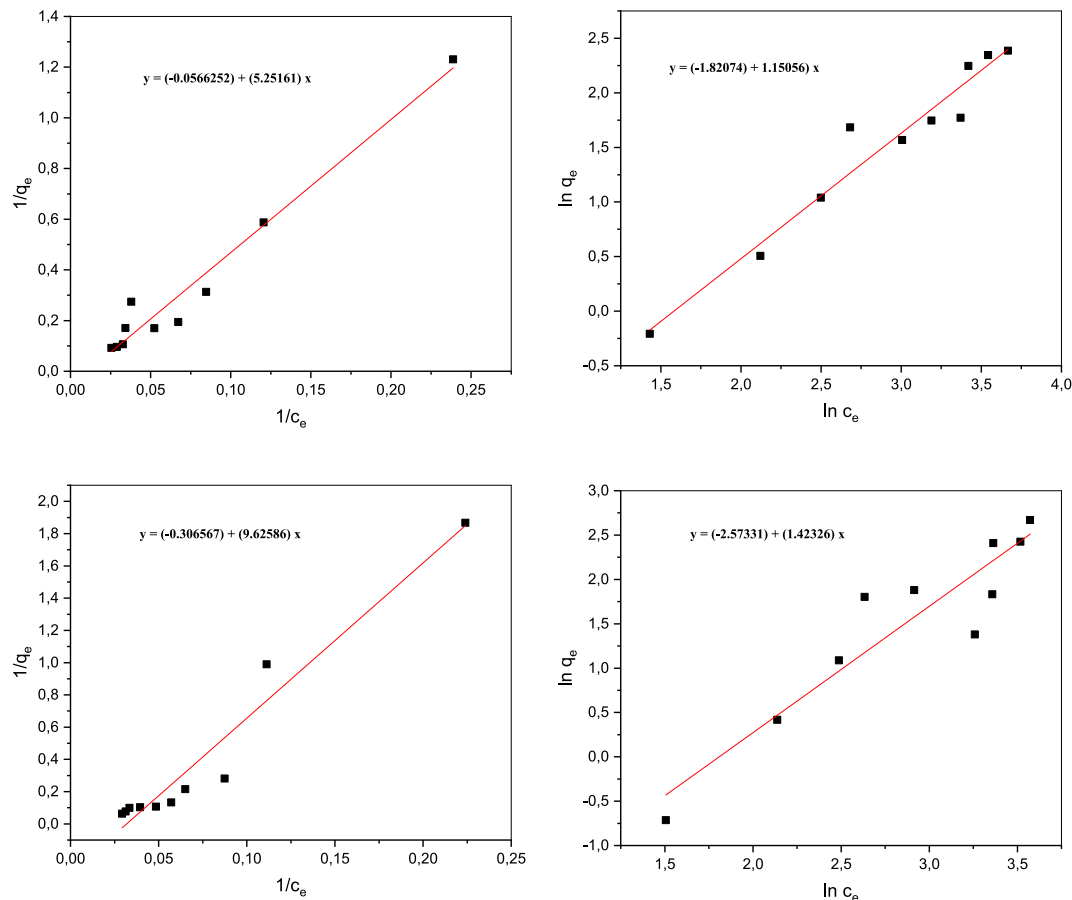


Fig. 4 Langmuir and Freundlich model at 35 °C (top) and 45 °C (bottom).

perimental data fit the Freundlich isotherm model. In addition, thermodynamic treatment of MB adsorption was performed at different temperatures; and related parameters ΔH , ΔS , and ΔG were measured. The results showed that the adsorption process of MB by CS-HA composite is spontaneous, and more favorable at low temperatures.

Acknowledgements: This work was supported by Universitas Jember through the Hibah Reworking Thesis/Skripsi funding.

REFERENCES

- Javed F, Rehman F, Khan AU, Fazal T, Hafeez A, Rashid N (2022) Real textile industrial wastewater treatment and biodiesel production using microalgae. *Biomass Bioenergy* **165**, 106559.
- Kadhom M, Albayati N, Alalwan H, Al-Furajji M (2020) Removal of dyes by agricultural waste. *Sustain Chem Pharm* **16**, 100259.
- Al-Ghouti MA, Al-Absi RS (2020) Mechanistic understanding of the adsorption and thermodynamic aspects of cationic methylene blue dye onto cellulosic olive stones biomass from wastewater. *Sci Rep* **10**, 15928.
- Pai S, Kini MS, Selvaraj R (2021) A review on adsorptive removal of dyes from wastewater by HA nanocomposites. *Environ Sci Pollut Res* **28**, 11835–11849.
- Ferreira WH, Silva LGA, Pereira BCS, Gouvêa RF, Andrade CT (2020) Adsorption and visible-light photocatalytic performance of a graphene derivative for methylene blue degradation. *Environ Nanotechnol Monit Manag* **14**, 100373.
- Bai N, Qi Y, Miu X, Yin J, Guo D, Wang J, Wang A (2023) Direct blending-drying method of graphitic carbon nitride (g-C₃N₄) with copper chloride solution for enhancement of photocatalytic decolorization of methylene blue. *ScienceAsia* **49**, 192–199.
- Serrano-Martínez A, Mercader-Ros MT, Martínez-Alcalá I, Lucas-Abellán C, Gabaldón JA, Gómez-López VM (2020) Degradation and toxicity evaluation of azo dye Direct red 83:1 by an advanced oxidation process driven by pulsed light. *J Water Process Eng* **37**, 101530.
- Suhan MBK, Shuchi SB, Anis A, Haque Z, Islam MS (2020) Comparative degradation study of remazol black B dye using electro-coagulation and electro-Fenton process: Kinetics and cost analysis. *Environ Nanotechnol Monit Manag* **14**, 100335.
- Beluci N de CL, Mateus GAP, Miyashiro CS, Homem NC, Gomes RG, Fagundes-Klen MR, Bergamasco R, Vieira AMS (2019) Hybrid treatment of coagulation/floccula-

- tion process followed by ultrafiltration in TIO_2 -modified membranes to improve the removal of reactive black 5 dye. *Sci Total Environ* **664**, 222–229.
10. Hashem AH, Saied E, Hasanin MS (2020) Green and ecofriendly bio-removal of methylene blue dye from aqueous solution using biologically activated banana peel waste. *Sustain Chem Pharm* **18**, 100333.
 11. Rai HS, Bhattacharyya MS, Singh J, Bansal TK, Vats P, Banerjee UC (2005) Removal of dyes from the effluent of textile and dyestuff manufacturing industry: A review of emerging techniques with reference to biological treatment. *Crit Rev Environ Sci Technol* **35**, 219–238.
 12. Benkhaya S, Mrabet S, Hsissou R, Harfi A (2020) Synthesis of new low-cost organic ultrafiltration membrane made from Polysulfone/Polyetherimide blends and its application for soluble azoic dyes removal. *J Mater Res Technol* **9**, 4763–4772.
 13. Rizkiana MF, Hidayatullah, Rosalina A, Fachri BA, Harada H (2021) Fabrication of magnetic activated carbon from spent coffee ground by hydrothermal synthesis for methylene blue removal. *IOP Conf Ser Mater Sci Eng* **1053**, 012007.
 14. Sawasdee S, Watcharabundit P (2022) Adsorption behavior and mechanism of alizarin yellow and rhodamine B dyes on water hyacinth (*Eichhornia crassipes*) leaves. *ScienceAsia* **48**, 804–812.
 15. Dutta S, Gupta B, Srivastava SK, Gupta AK (2021) Recent advances on the removal of dyes from wastewater using various adsorbents: A critical review. *Mater Adv* **2**, 4497–4531.
 16. Hynes NRJ, Kumar JS, Kamyab H, Sujana JAJ, Al-Khashman OA, Kuslu Y, Ene A, Kumar BS (2020) Modern enabling techniques and adsorbents based dye removal with sustainability concerns in textile industrial sector: A comprehensive review. *J Clean Prod* **272**, 122636.
 17. Rizkiana MF, Fachri BA, Gunawan S, Nor M, Iswahyono I, Palupi B, Rahmawati I, Amini HW (2023) Optimization of methylene blue ultrasound-assisted adsorption onto magnetic sugarcane bagasse activated carbon using response surface methodology. *Eng Chem* **2**, 43–51.
 18. Abdullah NH, Shameli K, Abdullah EC, Abdullah LC (2019) Solid matrices for fabrication of magnetic iron oxide nanocomposites: Synthesis, properties, and application for the adsorption of heavy metal ions and dyes. *Compos B Eng* **162**, 538–568.
 19. Duan C, Ma T, Wang J, Zhou Y (2020) Removal of heavy metals from aqueous solution using carbon-based adsorbents: A review. *J Water Process Eng* **37**, 101339.
 20. Hasan MM, Hasan MN, Awwal MR, Islam MM, Shenashen MA, Iqbal J (2020) Biodegradable natural carbohydrate polymeric sustainable adsorbents for efficient toxic dye removal from wastewater. *J Mol Liq* **319**, 114356.
 21. Mantasha I, Saleh HAM, Qasem KMA, Shahid M, Mehtab M, Ahmad M (2020) Efficient and selective adsorption and separation of methylene blue (MB) from mixture of dyes in aqueous environment employing a Cu(II) based metal organic framework. *Inorganica Chim Acta* **511**, 119787.
 22. Manatunga DC, de Silva RM, de Silva KMN, Ratnaweera R (2016) Natural polysaccharides leading to super adsorbent HA nanoparticles for the removal of heavy metals and dyes from aqueous solutions. *RSC Adv* **6**, 105618–105630.
 23. Fernando MS, Wimalasiri AKDVK, Dziemidowicz K, Williams GR, Koswattage KR, Dissanayake DP, de Silva KMN, de Silva RM (2021) Biopolymer-based nanohydroxyapatite composites for the removal of fluoride, lead, cadmium, and arsenic from water. *ACS Omega* **6**, 8517–8530.
 24. Agbabiaka OG, Oladele IO, Akinwekomi AD, Adediran AA, Balogun AO, Olasunkanm OG, Olayanju TMA (2020) Effect of calcination temperature on HA developed from waste poultry eggshell. *Sci Afr* **8**, e00452.
 25. Vidhya G, Kumar GS, Kattimani VS, Girija EK (2019) Comparative study of hydroxyapatite prepared from eggshells and synthetic precursors by microwave irradiation method for medical applications. *Mater Today Proc* **15**, 344–352.
 26. Alharby NF, Almutairi RS, Mohamed NA (2021) Adsorption behavior of methylene blue dye by novel crosslinked O-CM-chitosan hydrogel in aqueous solution: Kinetics, isotherm and thermodynamics. *Polymers* **13**, 3659.
 27. Rahmi, Ismaturrehmi, Mustafa I (2019) Methylene blue removal from water using H_2SO_4 crosslinked magnetic chitosan nanocomposite beads. *Microchem J* **144**, 397–402.
 28. Lei Y, Guan JJ, Chen W, Ke QF, Zhang CQ, Guo YP (2015) Fabrication of hydroxyapatite/chitosan porous materials for Pb(ii) removal from aqueous solution. *RSC Adv* **5**, 25462–25470.
 29. Lei Y, Chen W, Lu B, Ke QF, Guo YP (2015) Bioinspired fabrication and lead adsorption property of nanohydroxyapatite/chitosan porous materials. *RSC Adv* **5**, 98783–98795.
 30. Hassan MN, Mahmoud MM, El-Fattah AA, Kandil S (2016) Microwave-assisted preparation of nanohydroxyapatite for bone substitutes. *Ceram Int* **42**, 3725–3744.
 31. Hembrick-Holloman V, Samuel T, Mohammed Z, Jeelani S, Rangari VK (2020) Ecofriendly production of bioactive tissue engineering scaffolds derived from egg- and sea-shells. *J Mater Res Technol* **9**, 13729–13739.
 32. Nayak A, Bhushan B, Kotnala S (2022) Fabrication of chitosan-hydroxyapatite nano-adsorbent for removal of norfloxacin from water: Isotherm and kinetic studies. *Mater Today Proc* **61**, 143–149.
 33. Chandrasekaran A, Suresh S, Dakshanamoorthy A (2013) Synthesis and characterization of nanohydroxyapatite (n-HAP) using the wet chemical technique. *Int J Math Phys Eng Sci* **8**, 1639–1645.
 34. Ibrahim M, Abdel-Fattah WI, El-Sayed E-SM, Omar A (2013) A novel model for chitosan/hydroxyapatite interaction. *Quantum Matter* **2**, 234–237.
 35. Ibrahim M, Osman O, Mahmoud AA (2011) Spectroscopic analyses of cellulose and chitosan: FTIR and modeling approach. *J Comput Theor Nanosci* **8**, 117–123.
 36. Musah M, Azeh Y, Mathew JT, Umar MT, Abdulhamid Z, Muhammad AI (2022) Adsorption kinetics and isotherm models: A review. *Caliphate J Sci Technol* **4**, 20–26.
 37. Alsenani G (2021) Studies on adsorption of crystal violet dye from aqueous solution onto calligonum comosum leaf powder (CCLP). *J Am Sci* **17**, 70–75.